PROCEEDINGS OF SPIE

Design and testing of a low-resolution NIR spectrograph for the EXoplanet Climate Infrared TEIescope

Lee Bernard, Logan Jensen, John Gamaunt, Nat Butler, Andrea Bocchieri, et al.

SPIE.

Design and testing of a low-resolution NIR spectrograph for the EXoplanet Climate Infrared TElescope

Lee Bernard[1], Logan Jensen[1], Johnathan Gamaunt[1], Nat Butler[1], Andrea Bocchieri[2], Quentin Changeat[3], Azzurra D'Alessandro[13], Billy Edwards[3], Qian Gong[4], John Hartley[5], Kyle Helson[4, 12], Daniel P. Kelly[4], Kanchita Klangboonkrong[6], Annalies Kleyheeg[6], Nikole Lewis[7], Steven Li[5], Michael Line[1], Stephen F. Maher[4], Ryan McClelland[4], Laddawan R. Miko[4], Lorenzo V. Mugnai[2, 8], Peter Nagler[4], C. Barth Netterfield[9], Vivien Parmentier[10], Enzo Pascale[2], Jennifer Patience[1], Tim Rehm[6], Javier Romualdez[5], Subhajit Sarkar[11], Paul Scowen[4,1], Gregory S. Tucker[6], Augustyn Waczynski[4], and Ingo Waldmann[3]

[1]School of Earth and Space Exploration, Arizona State University, Tempe AZ, USA
[2]Department of Physics, La Sapienza Università di Roma, Roma, Italy
[3]Department of Physics, University College London, London, UK
[4]NASA Goddard Space Flight Center, Greenbelt MD, USA
[5]StarSpec Technologies Inc., Cambridge Ontario, Canada
[6]Department of Physics, Brown University, Providence RI, USA
[7]Department of Astronomy, Cornell Univ., Ithaca NY, USA
[8]INAF – Palermo Astronomical Observatory, Piazza del Parlamento, Italy
[9]Department of Physics, Univ of Toronto, Toronto Ontario, Canada
[10]Department of Physics, AOPP, Univ. of Oxford, Oxford, UK
[11]School of Physics and Astronomy, Cardiff Univ., Cardiff, UK
[12]Center for Space Sciences and Technology, University of Maryland, Baltimore MD, USA
[13]Centre for ExoLife Sciences, University of Copenhagen, Copenhagen, Denmark

ABSTRACT

The EXoplanet Climate Infrared TElescope (EXCITE) experiment is a balloon-borne, purpose-designed mission to measure spectroscopic phase curves of short-period extrasolar giant planets (EGPs, or "hot Jupiters"). Here, we present EXCITE's principal science instrument: a high-throughput, single-object spectrograph operating in the 0.8-2.5 μm and 2.5-4.0 μm bands with R$\geq$50. Our compact design achieves diffraction-limited, on-axis performance with just three powered optics: two off-axis parabolic mirrors and a CaF$_2$ prism. We discuss the optical and mechanical design, the expected optical performance of the spectrograph, and summarize the tolerances needed to achieve that performance. We also discuss plans for establishing alignment of the optics and verifying the optical performance.

Keywords: Exoplanet spectroscopy, hot Jupiters, balloon-borne instrumentation, infrared instrumentation

1. INTRODUCTION

The EXoplanet Climate Infrared TElescope (EXCITE) is a high-altitude long-duration balloon flight mission, purpose-designed to measure spectroscopic phase curves of short-period extrasolar giant planets (EGPs, or "hot Jupiters").[1,2] A general overview of the EXCITE experiment is given in these proceedings by Nagler et al.[3] Here, we discuss EXCITE's principal science instrument: a high-throughput, single-object spectrograph operating in the 0.8-2.5 μm and 2.5-4.0 μm bands with R$\geq$50. The compact design achieves diffraction-limited performance with just three powered optics: two off-axis parabolic mirrors (OAPs) and a CaF$_2$ prism. We discuss the expected optical performance of the spectrograph and summarizes the mechanical design. We also discuss plans for testing a prototype assembly, and lab-verification of alignment and optical performance at room temperature.

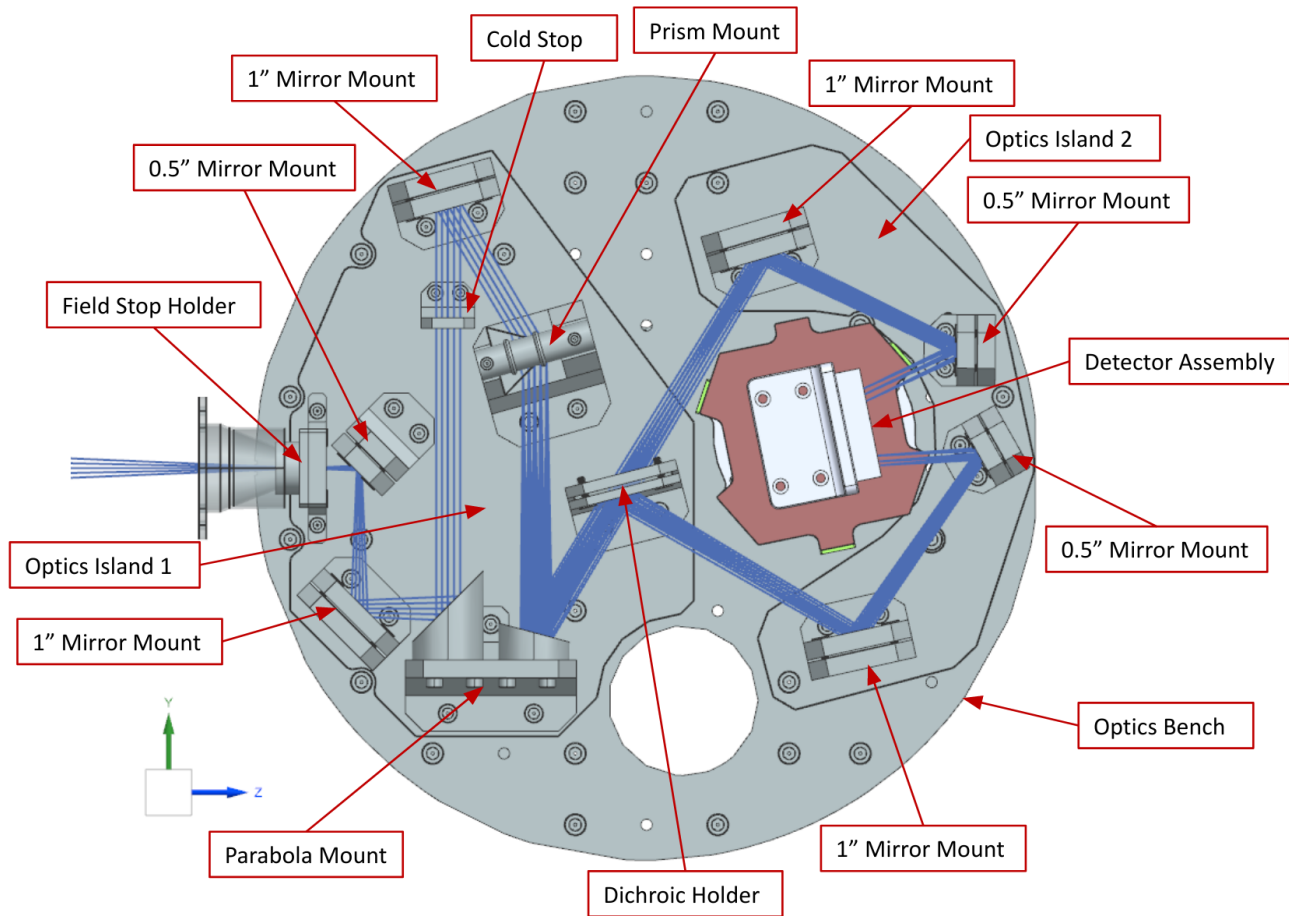Corresponding Author: Lee Bernard. E-mail: ldbernard@asu.edu

Figure 1: Top-down mechanical view of the EXCITE spectrograph. The optical bench is cooled by a 100 K cyrocooler stage, while the detector package is separately cooled by a 50 K cryocooler stage.[4] The mirror optics, field stop, and prism are commercial off-the-shelf parts, while the mounts, optics islands, and dichroic are custom-made. Note the OAPs are co-mounted, which simplifies the alignment.

1.1 Summary of the Spectrograph Design

EXCITE's spectrometer (**Figures 1, 2**), working on-axis, re-images a 100-micron wide field stop illuminated by a 0.5 m telescope producing a $f/12$ infrared (> 0.8 μm) beam. Cryogenic optics operating at 100 K collimate the beam, which is then directed through a cold stop to reduce stray light. A CaF_2 prism disperses the beam, and is then focused through a dichroic, splitting the beam into short and long wavelength channels. A short pass filter operating at 65 K in front of the detector package defines the band stop by eliminating light longward of 4.0 μm, and the focal plane is imaged by an H2RG detector. A 90° OAP with a focal length $f = 101.6$ mm (OAP 1) provides the collimation, and is followed by a 30° OAP with $f = 272.2$ mm (OAP 2) providing camera focus. The combination of the optics magnifies the beam ($f/32.2$ effective) to achieve near optimal spatial sampling at the detector, with fold mirrors maintaining a 30.5 cm (12 inch) diameter envelope. All mirrors are off-the-shelf parts.

1.2 Aberrations due to OAP Misalignment

Chang's "Geometrical Theory of Aberrations for Classical Offset Reflector Antennas and Telescopes"[5] provides an excellent resource for understanding the family of conic section optics, and we summarize here the relevant portions.
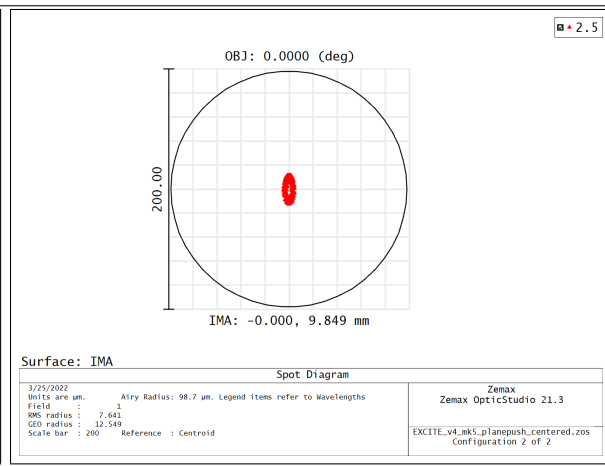
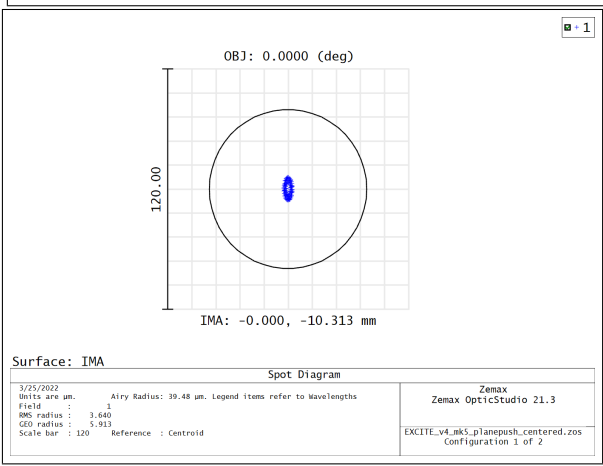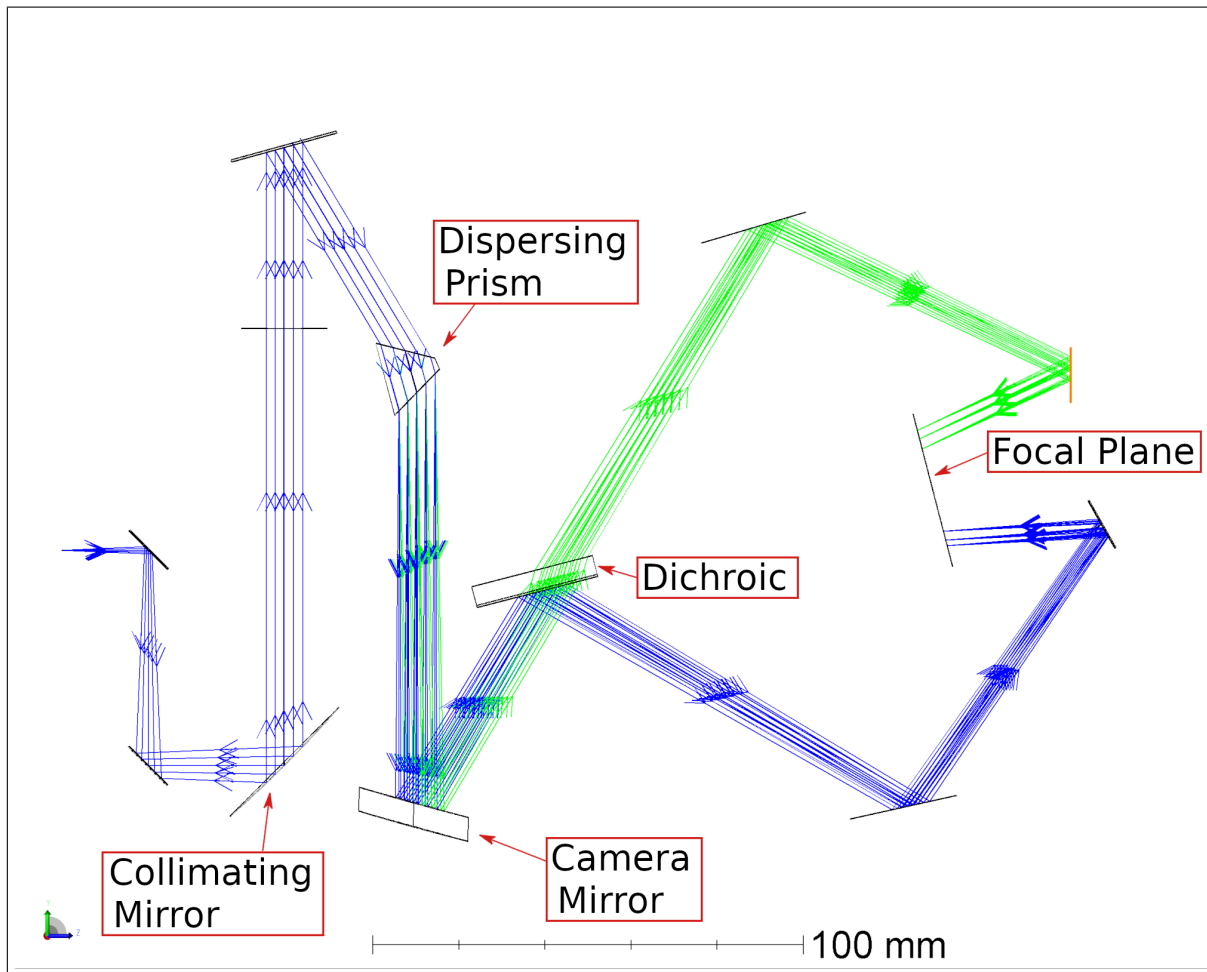**Figure 2: Top:** Zemax raytrace of the spectrograph, with the 0.8-2.5 μm channel in blue, and the 2.5-4.0 μm channel in green. **Left:** Focal plane spot from Zemax, for 1.0 μm light. Note the raytrace output is much smaller than the Airy disk (black circle). **Right:** Focal plane spot from Zemax, for 2.5 μm light. Note the change in scale: the Airy disk is now about 100 μm in radius.
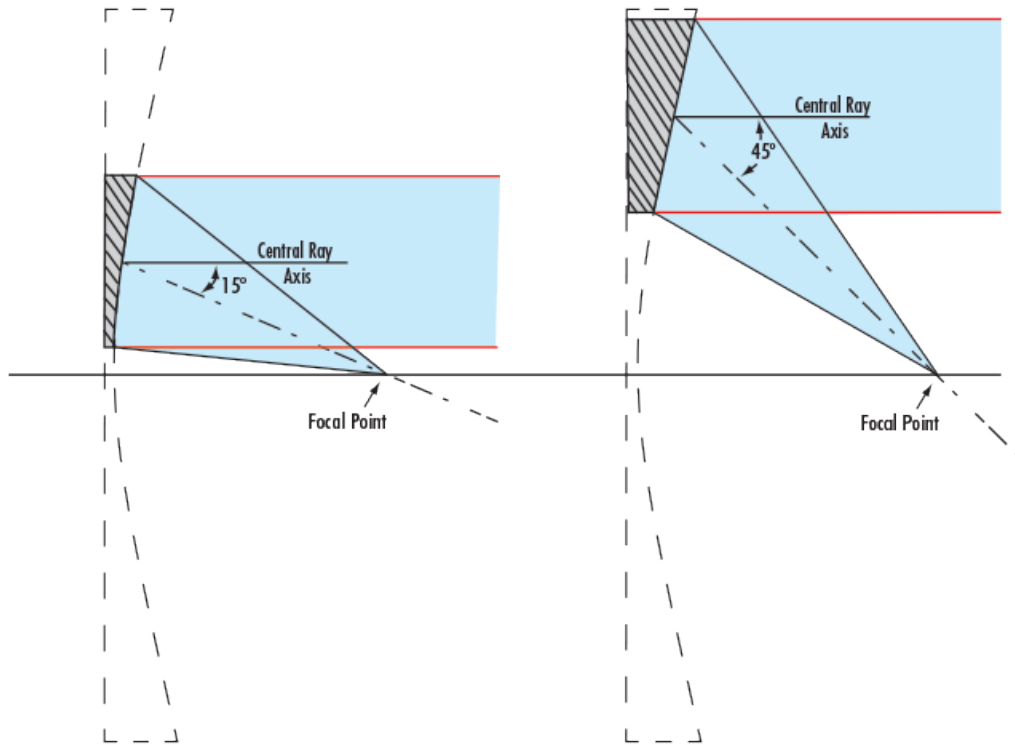
Figure 3: Example diagrams of OAP mirrors: a 15° OAP (Left), and a 45° OAP (Right). Image credit: edmundoptics.com

An OAP mirror is essentially a circular segment cut from a "parent" parabola (**Figure 3**), producing a versatile optic that, when used on-axis, is capable of focusing or collimating light in a single optical step with little to no aberration. OAPs are defined by two characteristics: the working angle, defined as the angle between the axis of focus and the axis of collimation (**Figure 3**); and the effective focal length, defined as the distance between the center of the OAP mirror and the focal point.

If the OAP is misaligned, it produces a defocus effect due to the focal plane rotating with the angle of the incoming rays. If the mirror is misaligned to the collimated beam (see **Figure 4**), it will effectively change the focal distance due to the the focal plane rotating with the angle of misalignment. However, the asymmetric nature of OAPs causes the tangential (e.g., horizontal) and sagittal (e.g., vertical) focal planes to rotate in opposite directions, producing a first order linear astigmatic aberration. For an OAP with working angle α and effective focal length s_0, the astigmatic focal lengths produced by a misalignment of angle θ is given by

$$\frac{1}{s_t} = \frac{1}{s_0}\Big(1 + \theta \tan\frac{\alpha}{2}\Big), \tag{1}$$

$$\frac{1}{s_s} = \frac{1}{s_0}\Big(1 - \theta \tan\frac{\alpha}{2}\Big), \tag{2}$$

where s_t is the tangential focal length, and s_s is the sagittal focal length. Note the $\pm\theta\tan(\alpha/2)$ term, this is the astigmatic tilting of the focal plane due to being off-axis from the parent parabola; as a consequence, the astigmatic aberration is modulated by the working angle of the OAP, with smaller working angles produces smaller aberrations. Also note that if working on-axis relative to the OAP (e.g., a perfectly aligned input beam with $\theta = 0$), the astigmatic term is eliminated, such that $s_t = s_s = s_0$.

If we maintain focus at s_0, this splits the difference between the tangential and sagittal focal planes. For small angles, this results in a symmetric, effectively defocused spot. The defocus distance d corresponds to the distance from s_0 to s_t/s_s. Using $d = s_0 - s_t = s_s - s_0$, and using the the small angle approximation, we can rearrange Equation 2 to relate the defocus d to the angle of misalignment θ:

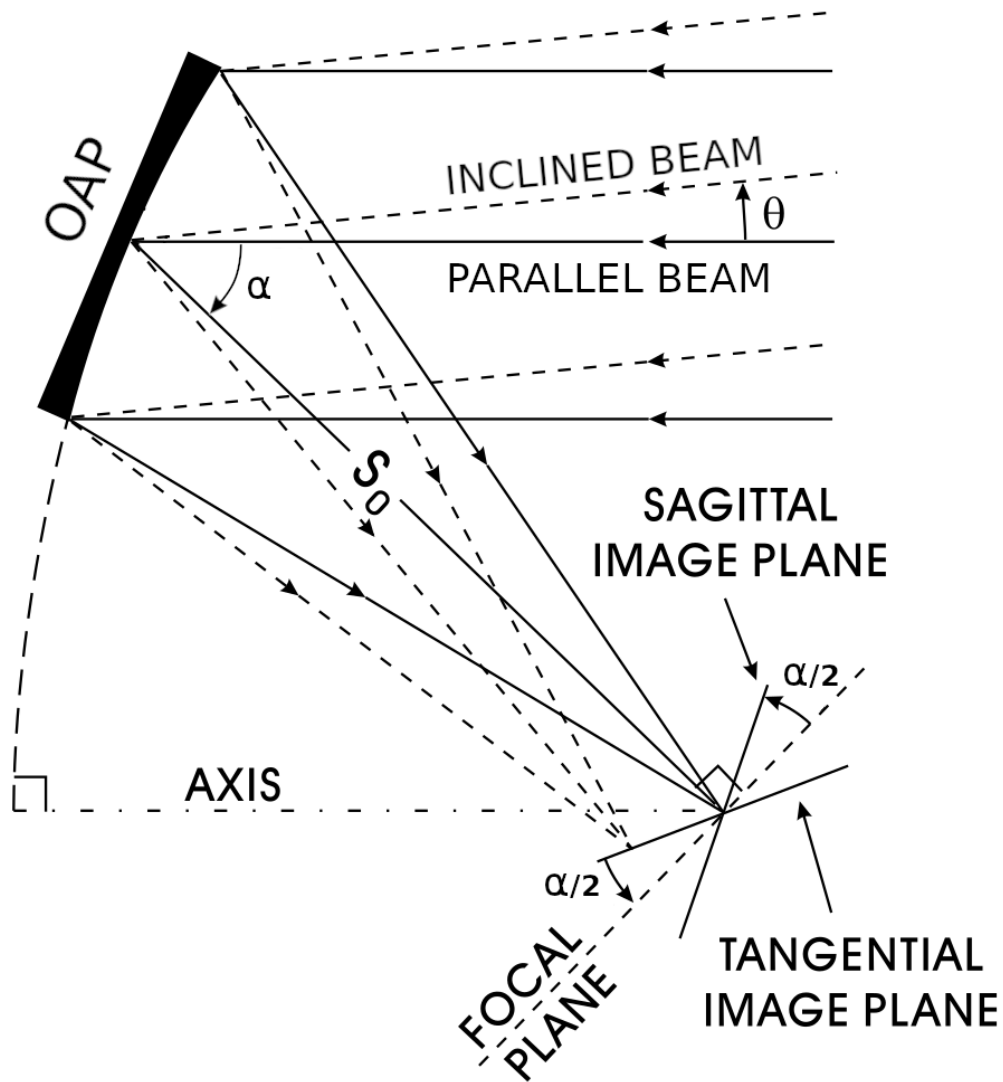**Figure 4:** Example diagram of an OAP with focal length s_0 and working angle α, illustrating the source of linear astigmatism. An on-axis beam is traced in solid lines, and an off-axis (or misaligned) beam is traced in dashed lines. Rays that enter the OAP off-axis by an angle θ converge at different focal points in the tangential and saggital image planes. Image credit: adapted from Chang (2003)[5]
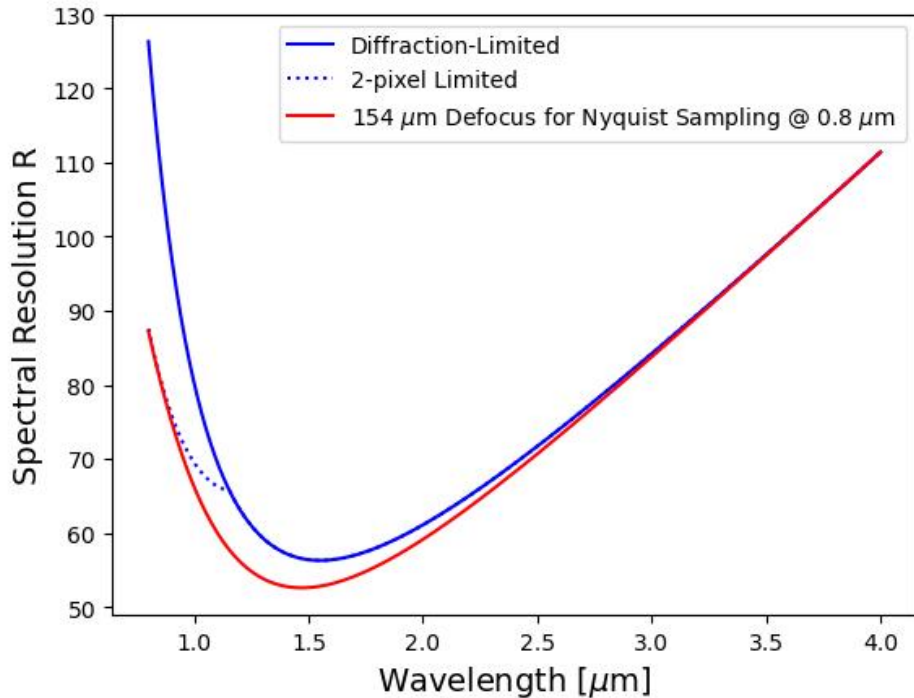
Figure 5: Theoretical spectral resolution R at the diffraction limit for the EXCITE spectrograph (blue curve). Also plotted (red curve) is the predicted resolution after a small telescope defocus that spreads the resolution element (FWHM) to two pixels at the shortest wavelength.

$$d \approx s_0 \theta \tan\frac{\alpha}{2}. \tag{3}$$

2. EXPECTED PERFORMANCE OF EXCITE SPECTROGRAPH

2.1 Performance Criteria

EXCITE operates at the diffraction limit, which we define as a Strehl ratio ≥ 0.8. The EXCITE spectrograph is effectively a "slit-less" spectrograph because the field stop (100 μm width) is significantly larger than the full width at half maximum (FWHM) of the telescope's diffraction-limited point spread function (PSF). Therefore, just as the FWHM at the diffraction limit defines signal width in the cross-dispersion direction in a typical slit-spectrometer (limiting signal-to-noise), the FWHM due to diffraction also defines EXCITE's spectral resolution ($R = 80$ predicted at 1 μm, $R \geq 50$ throughout the wavelength range; **Figure 5**).

The EXCITE $f/12$ telescope has a focal length $f = 6$ m and a central obscuration with outer radius equal to 0.38 times the primary mirror radius. Numerically, we find that the PSF set by diffraction has a FWHM equal to $0.96\lambda F$ at the telescope focus, where F is the focal ratio ($F = 12$). The collimating OAP (OAP 1) has a focal length of 101.6 mm, and the camera OAP (OAP 2) has a focal length of 272.2 mm, which yields a magnification of 2.7 and an effective focal ratio at the detector of $F = 32.2$. The FWHM of the PSF due to diffraction is then $r \sim 31$ μm, at a wavelength of 1 μm. Note, since the H2RG detector has a pixel pitch of 18 μm, this means we will be slightly under-sampled at 1 μm. In practice, the spectrograph will likely be operated with the telescope slightly out of focus to yield a FWHM of at least 2 pixels (see, **Figure 5**).

As explained in **Section 1.2**, alignment errors in the spectrograph - both displacements and rotations - yield defocused spots. To maintain diffraction-limited optical performance for EXCITE, we require the combination

of these defocus aberrations to be sufficiently small as to maintain the Strehl ratio. With the equations given in **Section 1.2**, we can calculate upper limits on focus and angular misalignment of the OAPs. For a given focus misalignment d, we find numerically that 0.8 Strehl corresponds to

$$d_{\mathrm{max}} = 0.74\lambda F^2. \tag{4}$$

Since the alignment tolerance increases with λ and $\lambda = 1~\mu$m is near the blue end of our spectrum, we take $\lambda = 1$ μm as the reference wavelength for alignment purposes. We then use **Equation 4** combined with **Equation 3** to calculate the angular tolerance θ:

$$\theta_{\mathrm{max}} = \frac{0.74\lambda F^2}{f\tan\frac{\alpha}{2}}. \tag{5}$$

2.1.1 Performance Tolerances

Using **Equations 4** and **5** we can calculate the tolerances of the OAPs. Since the input telescope beam is $F = 12$, the total defocus budget at the 90° OAP is 108 μm. Assuming the system is in focus, we calculate the angular tolerance of the 90° OAP to be 3.7 arcmins. Therefore, the 90° OAP has a combined tolerance of $\sim$100 μm in linear alignment and $\sim$3.7 arcmins in angular alignment.

For the 30° OAP, our calculated tolerances are $\sim$790 μm in linear alignment and 37 arcmins in angular alignment. Note the tolerances of the 30° OAP are signifigantly relaxed compared to the 90° OAP. This is partially due to the the telescope beam being magnified to $F = 32.2$ by the 30° OAP, and partially due to the OAP's shallower working angle of 30°. The principle reason for choosing a shallow 30° working angle for OAP 2 is to relax the angular tolerances associated with the $\pm$0.5 degree angular deviation from on-axis resulting from dispersion by the prism, preserving diffraction-limited performance across the wavelength range.

To aid in the combined alignment effort of two OAP mirrors, we have written a simple raytrace program in Python (**Figure 6**) which generates spot diagrams given a range of input misalignments. This allows us to rapidly diagnose likely misalignments causing elongated point source images in the real spectrograph.

We note that telescope jitter is expected to produce variations at the focal plane of <0.3 px (5.4 μm),[2] and at EXCITE's high altitude ($\sim$ 40 km) seeing is negligible, so the diffraction limit dominates the spot size at the detector focal plane.

3. LAB EQUIPMENT AND PROTOTYPING

Current laboratory work is focused on validating the spectrograph design and developing techniques for aligning the optics. We have developed a prototype spectrograph that is nearly optically-equivalent to the final spectrograph. We will assemble OAPs 1 and 2 in the configuration shown in the design (**Figure 1**), and use a visible-light laser to perform alignment. We will then validate alignment at longer wavelengths according to the criteria given in **Section 2.1**, as measured by an infrared detector. Due to the achromatic nature of mirrors, alignment should be wavelength independent. The tolerances also increase with increasing wavelength, making baseline alignment at a short wavelength desirable.

As more optical parts arrive, such as the dichroic, we will add them to the prototype and validate their performance. Because our laboratory infrared detector (InGaAs, cutoff 1.7 μm) cannot cover the full wavelength range of EXCITE and we will not have access to EXCITE's detector until integration of the subsystems, we cannot directly confirm spectrometer performance at longer wavelengths. We have developed a work-around by making use of a monochromator and broad-band infrared photo-diode. Where we cannot check alignment, we can use the photo-diode to measure throughput of the spectrograph system, validating the prototype for all wavelengths, and validating that the dichroic separates the two channels.
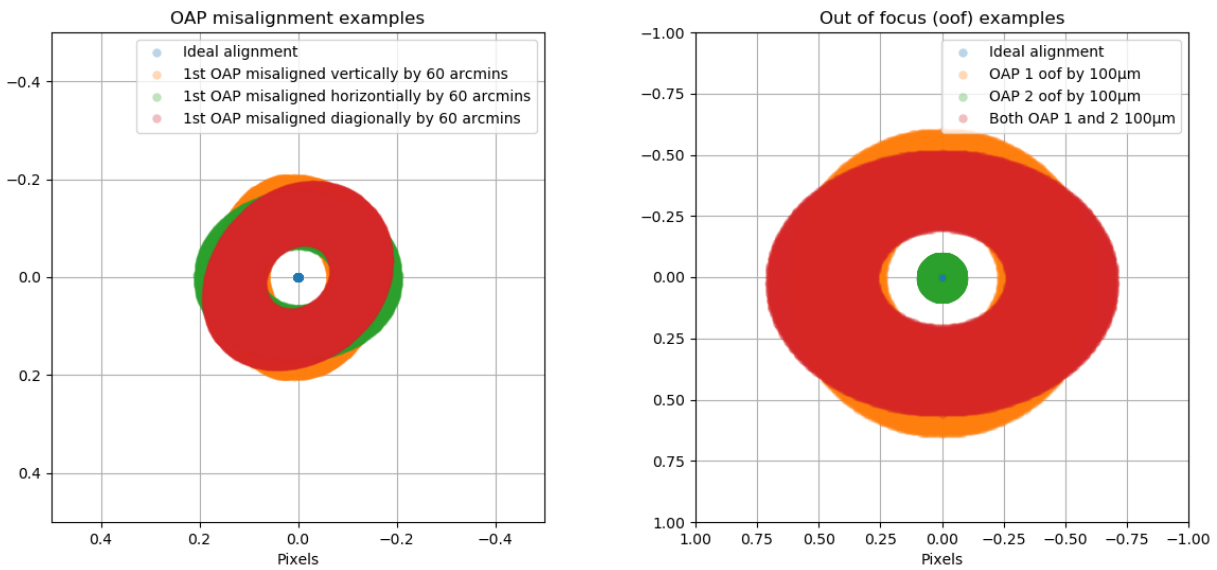
Figure 6: Ray-trace simulations for the two OAP system ignoring diffraction (in pixels). **Left:** Examples of angular misalignment of OAP 1 with rotations in various directions. **Right:** Examples of misalignment in the two-OAP system. A rotation of OAP 1 can be compensated for by a defocus of OAP 2 (and vice versa), but other misalignments do not compensate and tend to produce elongated spot diagrams.
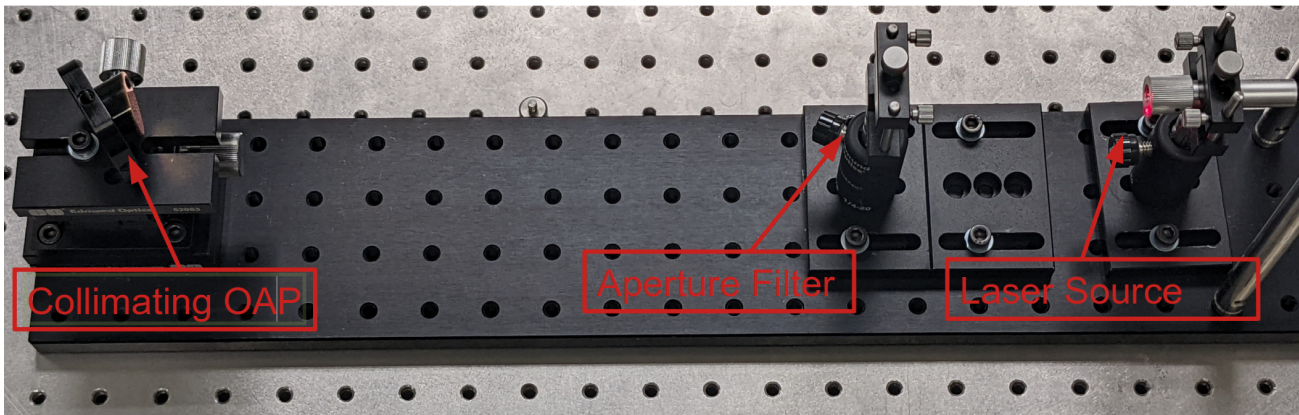

Figure 7: Collimated 650 nm laser light source, utilizing a 10 μm aperture for spacial filtering and a 30° OAP mirror.
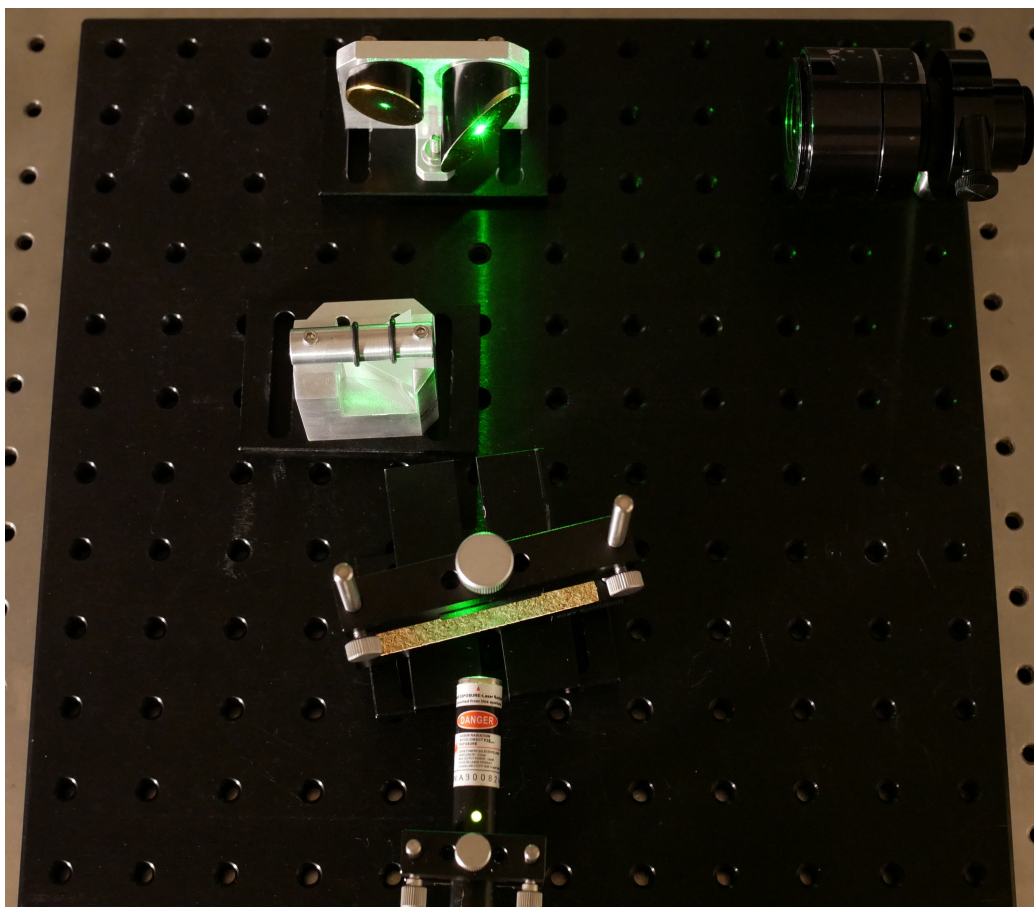
Figure 8: Prototype layout, with green laser light for demonstration purposes. We input light from the collimation direction, and then reflect that light back through the system to perform auto-collimation tests.

3.1 Prototype Illumination Source

The first step in prototype testing was building an optical source for measuring the alignment of EXCITE's spectrometer. For initial testing and prototyping, we decided on making use of a combination of a laser, aperture, and an OAP to produce a collimated light source. (See **Figure 7** for the layout.) The illumination source is a Thorlabs 650 nm laser focused to a ≈ 30 μm spot. We place a 10 μm aperture at the laser focus, to filter out beam structure. The output of the aperture is collimated by a $30°$ OAP with a 272.2 mm effective focal length. By placing the OAP on a translation stage, we are able to fine tune the focus of the OAP relative to the aperture and achieve a highly collimated beam. The collimated output can then be used to test spectrograph optics.

3.2 Plans for alignment and verification

We have begun testing a novel approach to demonstrate alignment of the spectrograph (e.g., Figure 8). First, we direct collimated light through a 50/50 beam splitter and into the collimating mirror, operating OAP 1 in reverse. We then place a mirror at the focal point of OAP 1, and reflect light back through the system. By ensuring the reflected beam is aligned with the input beam, we can autocollimate the system. The 50/50 beam splitter then directs the reflected collimated beam into the prism, and from there into the camera focus mirror (OAP 2). Between the beam splitter and the prism, we will measure the output of the collimated beam via a shear plate interferometer. Once the spectrograph has been aligned, we will replace the beam splitter with the appropriate fold mirror, and re-perform alignment of that fold mirror with conventional slit illumination. Using this system, we can measure both the focus and collimation alignment of the collimating OAP, which as shown in Section 2.1 is the highest tolerance task, independently from the rest of the spectrograph.

Because of their reduced tolerances, the alignment of subsequent optics – including the camera mirror – is largely independent from the first OAP. Once the collimating OAP has been aligned, we will add and align the next optic, iterating through each part in turn until spectrograph is complete. During this process, we will use a blank dichroic substrate, enabling use to align both channels with the visible laser light. Finally, we note that while alignment is being performed with warm optics, our initial thermal modeling indicates that alignment will be maintained within the tolerances given in **Section 2.1** after cooling to the operating temperature of 100 K.

4. CONCLUSIONS

We have developed optical and mechanical designs for the EXCITE spectrograph. Additionally, we have defined spectrograph alignment tolerances, and we have the mathematical framework to quantify spectrograph alignmentment from measurable observables. We have developed a prototype of the spectrograph as well as laboratory tools to support testing and alignment, including a simulation that can be used for rapid diagnosis of abberations. And finally, we have a plan for verifying the performance of the design via a novel technique. This positions us well to move on to building and aligning the flight spectrograph.

ACKNOWLEDGMENTS

REFERENCES

[1] G. S. Tucker, P. Nagler, N. Butler, B. Kilpatrick, A. Korotkov, N. Lewis, P. F. L. Maxted, L. Miko, C. B. Netterfield, E. Pascale, J. Patience, P. Scowen, V. Parmentier, I. Waldmann, and Y. Wen, "The Exoplanet Climate Infrared TElescope (EXCITE)," in *Ground-based and Airborne Instrumentation for Astronomy VII*, H. Takami, C. J. Evans, and L. Simard, eds., p. 199, SPIE, (Austin, United States), July 2018.

[2] P. C. Nagler, B. Edwards, B. Kilpatrick, N. K. Lewis, P. Maxted, C. B. Netterfield, V. Parmentier, E. Pascale, S. Sarkar, G. S. Tucker, and I. Waldmann, "Observing Exoplanets in the Near-Infrared from a High Altitude Balloon Platform," *Journal of Astronomical Instrumentation* **08**, p. 1950011, Sept. 2019.

[3] P. C. Nagler, L. Bernard, A. Bocchieri, N. Butler, Q. Changeat, A. D'Alessandro, B. Edwards, J. Gamaunt, Q. Gong, J. Hartley, K. Helson, L. Jensen, D. P. Kelly, K. Klangboonkrong, A. Kleyheeg, N. K. Lewis, S. Li, M. Line, S. F. Maher, R. McClelland, L. R. Miko, L. V. Mugnai, B. Netterfield, V. Parmentier, E. Pascale, J. Patience, T. Rehm, J. Romualdez, S. Sarkar, P. A. Scowen, G. S. Tucker, A. Waczynski, and I. Waldmann, "The Exoplanet Climate Infrared TElescope (EXCITE)," *these proceedings*, 2022.

[4] T. Rehm, L. Bernard, A. Bocchieri, N. Butler, Q. Changeat, A. D'Alessandro, B. Edwards, J. Gamaunt, Q. Gong, J. Hartley, K. Helson, L. Jensen, D. P. Kelly, K. Klangboonkrong, A. Kleyheeg, N. K. Lewis, S. Li, M. Line, S. F. Maher, R. McClelland, L. R. Miko, L. V. Mugnai, P. C. Nagler, B. Netterfield, V. Parmentier, E. Pascale, J. Patience, J. Romualdez, S. Sarkar, P. A. Scowen, G. S. Tucker, A. Waczynski, and I. Waldmann, "The design and development status of the cryogenic receiver for the EXoplanet Climate Infrared TElescope," *these proceedings*, 2022.

[5] S. Chang, "Geometrical Theory of Aberrations for Classical Offset Reflector Antennas and Telescopes," *https://www.researchgate.net/publication/234505990 [Doctoral dissertation, University of Southern California.]* , p. 87, 2003.